INORGANIC CHEMISTRY FRONTIERS

CCS 中国化学会 CHINESE CHEMICAL SOCIETY

ROYAL SOCIETY OF CHEMISTRY

A Selenium-Based "Alkahest": Reactive Dissolutions of Metals and Metal Compounds with n-Alkylammonium Polyselenide Solutions

Journal:	*Inorganic Chemistry Frontiers*
Manuscript ID	QI-RES-08-2023-001632
Article Type:	Research Article
Date Submitted by the Author:	16-Aug-2023
Complete List of Authors:	Turnley, Jonathan; Purdue University, Davidson School of Chemical Engineering Deshmukh, Swapnil; Purdue University, Chemical Engineering Boulos, Victoria; Purdue University System, Chemistry Spilker, Robert; Purdue University, Breckner, Christian; Purdue University, Davidson School of Chemical Engineering Ng, Kevin; Purdue University, Chemical Engineering Liu, Judy; Purdue University System, Chemistry Miller, Jeffrey; Purdue University Kenttamaa, Hilkka; Department of Chemistry, Purdue University Agrawal, Rakesh; Purdue University,

ARTICLE

A Selenium-Based "Alkahest": Reactive Dissolutions of Metals and Metal Compounds with n-Alkylammonium Polyselenide Solutions

Received 00th January 20xx,
Accepted 00th January 20xx

DOI: 10.1039/x0xx00000x

Jonathan W. Turnley,[a] Swapnil D. Deshmukh,[a] Victoria M. Boulos,[b] Robert Spilker,[a] Christian J. Breckner,[a] Kevin Ng,[a] Judy Kuan-Yu Liu,[b] Jeffrey T. Miller,[a] Hilkka I. Kenttämaa,[b] and Rakesh Agrawal*[a]

The solution-processing of metal chalcogenides offers a promising route to improve the manufacturing of semiconductor devices. The amine-thiol solvent system has been deemed an "alkahest" for its ability to dissolve a wide range of metals and metal chalcogenides. Therefore, it enables convenient synthesis of metal sulfides. However, in the literature there are limited reports of analogous selenium-based "alkahest" chemistry. Here we show that solutions containing n-alkylammonium polyselenides can dissolve a wide range of metals and metal compounds through the formation of soluble metal polyselenides. These metal polyselenides can subsequently be utilized as precursors for the synthesis of a wide range of binary and multinary metal selenide thin films and nanoparticles, including $Cu(In,Ga)Se_2$, $Cu_2ZnSnSe_4$, and $Ag_2ZnSnSe_4$.

Introduction

Metal selenide semiconductors are a versatile class of materials with a wide range of applications, including photovoltaics, thermoelectrics, light emitting diodes, and transistors.[1–4] The solution-based deposition methods used to generate these materials offer great promise in reducing costs, increasing throughput, and improving materials usage efficiency compared to vacuum deposition methods.[5,6] Direct dissolution of the desired metal chalcogenide semiconductor in a simple solvent is often difficult, leading to the use of soluble metal halides, nitrates, and acetylacetonates as precursors.[7] The metal salts are then allowed to react with a soluble selenium compound. Common selenium sources include sodium selenite, selenourea, selenium chloride, and trioctylphosphine selenide.[8–11] However, the use of these metal salts can lead to challenges caused by anionic impurities.[12] For example, oxygen containing anions can lead to the formation of metal oxide secondary phases[13] and halide anions have been observed to incorporate into metal chalcogenide crystal latices, affecting the optoelectronic properties.[14]

One route to avoid anionic impurities is to utilize metal complexes that contain metal-selenium bonds. This may allow the precursors to decompose directly into the target compounds without needing to react with an external selenium source. A wide variety of single source precursors for metal selenides have been investigated, including diselenophosphinate, diselenocarbamate, and selenolate complexes.[15] Of particular relevance to this work are metal complexes containing polyselenide ligands. A wide variety of metal complexes containing polyselenide ligands have been identified and they are often soluble in polar solvents.[16] Generally, these species contain a metal polyselenide anion with a large selenium-to-metal ratio that is stabilized by large organic cations.[17] Furthermore, these organic metal polyselenides have been successfully used in the solution synthesis of metal selenide materials, including $CuInSe_2$.[18] One challenge for these metal-selenium bonded complexes is that they often rely on a complex synthesis process, which could negatively impact the ability to utilize these precursors at an industrial scale. For example, the synthesis of organic metal polyselenides has historically relied on the initial synthesis of sodium polyselenide by a reaction of elemental sodium and selenium in liquid ammonia. Subsequently, the sodium polyselenide can be allowed to react with an organic chloride and a metal chloride, forming the organic metal polyselenide in solution and precipitating sodium chloride.[19]

To facilitate the synthesis of soluble metal complexes that contain metal-chalcogen bonds, several reactive solvent systems have been developed. This reactive dissolution chemistry has been covered in depth in recent review articles.[20,21] These solvent systems are capable of dissolving a wide range of metal precursors by reactions that form soluble metal complexes, in some cases even directly dissolving metal chalcogenides and metals.[22,23]

The combination of hydrazine and a chalcogen is capable of dissolving several metal chalcogenides, including Cu_2S, SnS_2, In_2Se_3, and ZnTe.[22] Investigation into this dissolution chemistry has identified the formation of hydrazinium chalcogenidometallates.[24] These soluble metal complexes have then been shown to decompose cleanly upon heating, allowing

[a] Davidson School of Chemical Engineering, Purdue University, West Lafayette, Indiana 47907, United States
[b] Department of Chemistry, Purdue University, West Lafayette, Indiana 47907, United States

Electronic Supplementary Information (ESI) available: [details of any supplementary information available should be included here]. See DOI: 10.1039/x0xx00000x

for the formation of the desired metal chalcogenide semiconductors.[25] To this end, the hydrazine-chalcogen solvent system has been used to fabricate solution-processed $Sn(S,Se)_2$ transistors, $Cu(In,Ga)(S,Se)_2$ solar cells, and $Cu_2ZnSn(S,Se)_4$ solar cells.[26–28] However, hydrazine is both highly toxic and explosive, potentially hindering the scale-up of this chemistry necessary for commercial production.

The amine-thiol reactive solvent system has been proposed as an alkahest (or universal solvent) for its ability to dissolve a wide range of precursors.[29] Research has shown that different combinations of an amine and a thiol allow for this reactive solvent system to dissolve a wide range of metals (Cu, Zn, In, Ga, Sn, Sb), chalcogenides (S, Se, Te), and metal chalcogenides (CuS, Cu_2S, Ag_2S, Ag_2Se, In_2Se_3, SnS, SnSe, As_2S_3, As_2Se_3, As_2Te_3, Sb_2S_3, Sb_2Se_3, Sb_2Te_3, Bi_2S_3, Bi_2Se_3, Bi_2Te_3).[30,31] As a variant, simple thiols can be replaced with thioglycolic acid (TGA), which contains both a thiol and carboxylic acid functional groups. TGA-amine solutions have similarly been shown to be a reactive solvent system.[32,33] Or the thiols can be replaced with 2-mercaptoethanol, which has both a thiol and an alcohol group, to achieve a reactive solvent system.[34]

Zhao et al. studied the dissolution of Cu and In metals in monoamine-dithiol solutions and discovered the formation of chelated metal thiolates.[23] The presence of the metal-sulfur bond in the metal thiolates is convenient in the pursuit of solution-processed metal sulfides as Deshmukh et al. showed that these metal thiolates cleanly decompose into the respective metal sulfides.[35] However, this poses a challenge for fabricating sulfur-free metal selenides. Although the amine-thiol solvent system can dissolve metal selenides and selenium, the thiol is still present to potentially act as a sulfur.[36] Depending on subsequent annealing conditions, the formation of sulfoselenide materials rather than selenides can occur.[37] While in some cases sulfur alloying into a metal selenide material is beneficial, in other cases the pure selenide material is desired. For example, sulfur content in solution-processed $Cu(In,Ga)(S,Se)_2$ precursor films has been linked to challenges with grain growth.[36] Therefore, alternative methods are needed for sulfur-free, solution-processed metal selenides, preferably utilizing a selenium-based alkahest.

To date there is limited work on alkahest chemistry that is sulfur-free and can produce metal selenides. This type of processing is limited to certain metal selenides that can dissolve in presence of hydrazine and selenium and some examples of reactive dissolutions of metals with organic diselenides.[22,38]

In this work, we present n-alkylammonium polyselenide solutions as a versatile, selenium-based reactive solvent system. These n-alkylammonium polyselenides ($(RNH_3)_2Se_x$) are simple to synthesize and can dissolve numerous pure metals, metal selenides, metal oxides, and metal salts through the formation of soluble metal polyselenides. Therefore, these metal polyselenides offer a generalized sulfur-free route to solution processed metal selenide semiconductors.

Experimental

Materials

Copper (99.999%), gallium (99.9999%), silver (99.9%), germanium (99.999%), bismuth (99.99%), antimony (99.995%), arsenic (99.997%), selenium powder (100 mesh, 99.99%), selenium pellets (99.995%), copper(I) selenide (99.95%), copper(I) oxide (99.99%), copper(I) chloride (99.995%), indium(III) chloride (99.999%), n-butylamine (BA; 99.5%), n-propylamine (PA; 99%), n-hexylamine (HA; 99%), oleylamine (technical grade, 70%) 1,2-ethanedithiol (EDT; 98%), hydrazine (anhydrous, 98%), toluene (anhydrous, 99.8%), cyclohexane (anhydrous, 99.5%), N-methyl-2-pyrrolidone (NMP) (anhydrous, 99.5%), deuterated dimethyl sulfoxide (99.96 atom % D), and ethylene carbonate (99.96%) were purchased from Sigma Aldrich. Trace-metal grade nitric acid, indium (99.999%), tin (99.999%), and indium(III) selenide (99.99%) were purchased from Fisher. Zinc (99.9%), lead (99.95%), and cadmium (99.99%) were purchased from Alfa Aesar. Ethanethiol (ET; 99%) was purchased from Acros Organics. Before use, Gallium had surface oxide removed via scrapping with a knife. Oleylamine was degassed through three freeze-pump-thaw cycles. All other materials were used as received. All materials were stored in a glovebox under nitrogen atmosphere.

Preparation and isolation of n-alkylammonium polyselenides

The preparation of n-alkylammonium polyselenides was performed in a glovebox under a nitrogen atmosphere. A schematic of this procedure is shown in Figure 1. Selenium powder was dissolved in a n-butylamine and ethanethiol solution at a Se:BA:ET mol ratio of 1:2:2 on a stir plate. For n-hexylammonium polyselenide and n-propylammonium polyselenide, the same procedure was used while replacing BA with n-hexylamine or n-propylamine. The n-alkylammonium polyselenides were isolated via precipitation and centrifugation. Briefly, about 700 µL selenium-amine-thiol solution was combined with an antisolvent composed of 20 mL toluene and 1 mL cyclohexane. The resulting solid precipitate was isolated via centrifugation at 14,000 rpm for 5 minutes followed by decanting the supernatant and drying under vacuum for 2 minutes. The dried complex was then redissolved in 250 µL of the same pure amine that was used in the initial selenium dissolution. The complex was again isolated by the same procedure with an additional 15 minutes of drying. The resulting n-alkylammonium polyselenide solid was then redissolved in either amines or polar solvents like dimethyl sulfoxide or dimethylformamide. For hydrazinium polyselenide, no precipitation was needed as hydrazine produced polyselenide ions upon dissolution of selenium and there were no sulfur containing species present that needed to be separated. The hydrazinium polyselenide solutions were used directly.

Preparation of n-alkylammonium metal polyselenides and synthesis of metal selenides

The preparation of metal polyselenides was carried out in a glovebox under a nitrogen atmosphere. Isolated n-butylammonium polyselenide was dissolved in n-butylamine at a selenium concentration of approximately 0.5 M. The metal

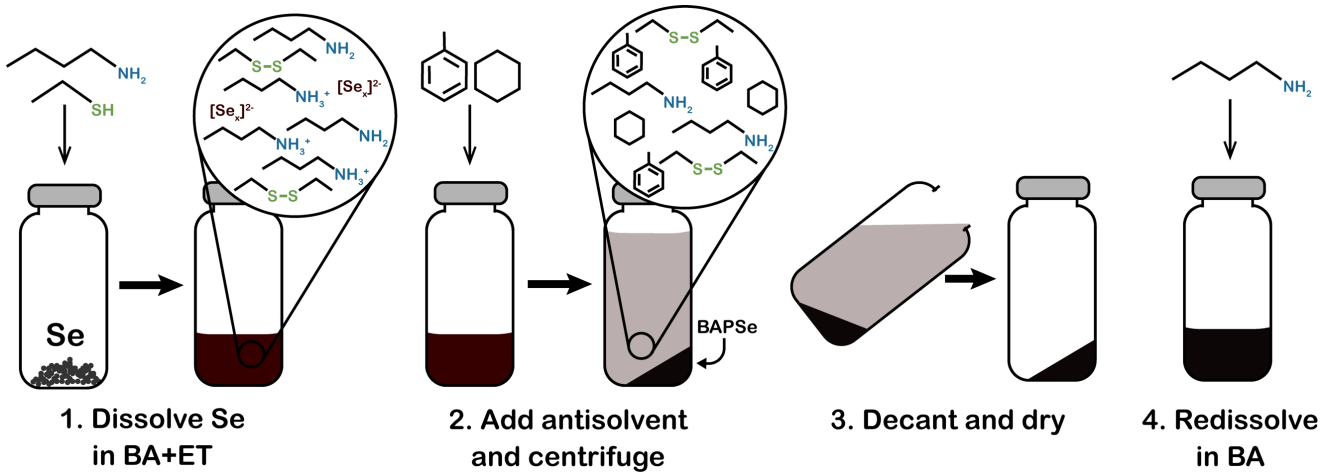

Figure 1. Schematic outlining the synthesis of butylammonium polyselenide (BAPSe) solutions starting by dissolving selenium in n-butylamine (BA) and ethanethiol (ET), precipitating out the BAPSe with antisolvent addition and centrifugation, decanting the supernatant, drying, and redissolving in BA. For multiple washing cycles, steps 2-4 can be repeated.

precursor was then added into the solution at a Se:metal mol ratio of 10:1 and stirred at 35 °C on a heated stirplate. Copper dissolved in a matter of hours, while indium dissolved in 1-2 days. Other metals were allowed to dissolve over the course of several weeks. Arsenic and tin appeared to be fully dissolved but other metals still had solid residue remaining. Silver fully dissolved when using a Se:Ag mol ratio of 20:1. For bismuth, lead, and antimony, more solid residues were observed than was initially present, suggesting the occurrence of a reaction that formed a solid product. The solutions were centrifuged before use to separate out solid materials. Solutions were drop-cast and annealed between 300 °C and 400 °C for 5 minutes.

For $CuInSe_2$ inks, the respective metal solutions were combined and films were blade coated onto Mo-coated sodalime glass. For each layer, the film was annealed between 300-350 °C for 2-5 min. The film was then heated to 500 °C for 20 min in a tube furnace with no additional selenium.

For $Cu(In,Ga)Se_2$, $Cu_2ZnSnSe_4$, and $Ag_2ZnSnSe_4$ inks, the respective metal solutions were combined at appropriate ratios based on the stoichiometry of the targeted multinary metal selenide. $Cu(In,Ga)Se_2$ and $Cu_2ZnSnSe_4$ films were annealed at 400 °C for 5 minutes and the $Ag_2ZnSnSe_4$ film was annealed at 250 °C for 10 minutes.

For $CuInSe_2$ nanoparticles, the copper and indium polyselenides were isolated via precipitation with toluene and redissolved in oleylamine. The solution was then allowed to react at 225 °C for 30 minutes in a Biotage Initiator Microwave Reactor. Excess selenium was removed by dissolving in a mixture of oleylamine and ethanethiol. The remaining solid particles were washed twice. This was achieved by isolating the particles via centrifugation with isopropanol as an antisolvent and decanting the supernatant. For the second washing cycle, the particles were redispersed in hexanes and the isolation procedure was repeated.

$CuInSe_2$ Solar Cell Fabrication

Devices were constructed with an architecture of SLG/Mo/CISe/CdS/ZnO/ITO/Ni/Al. Mo was deposited onto sodalime glass via sputtering to a thickness of 800 nm. The $CuInSe_2$-ink was modified to minimize the Se/metal ratio while not becoming too viscous. This was done by separately making an In and Cu inks. The In ink contained In in BAPSe+BA with an In:Se ratio of 1:6 and an In concentration of 0.33 M. The Cu ink contained Cu_2Se in BAPSe+BA with a Cu_2Se:Se ratio of 1:12 and a Cu concentration of 0.3 M. The inks were then combined for a Cu:In ratio of 0.95:1. The combined ink was blade coated onto the Mo-coated substrate. The samples were annealed at temperatures between 300-350 °C for 2 minutes each layer. In total, 20 layers were coated. Heat treatment under a Se atmosphere was performed in an Ar-purged tubular furnace with films placed in a rectangular graphite box and surrounded with 500-600 mg of crushed selenium pellets. The furnace was preheated to 510 °C before film insertion, and films were left in for 20 minutes before the furnace is opened and allowed to cool naturally. After selenization, ~50 nm of CdS were deposited via chemical bath deposition using $CdSO_4$, NH_4OH, and thiourea. Chemical vapor deposition was used to deposit 50 nm ZnO followed by 150 nm ITO. Last, cut masks were used to deposit 100 nm Ni followed by 1000 nm Al in a grid shape via electron beam evaporation.

Characterization

Raman spectroscopy and photoluminescence (PL) spectroscopy were performed using a Horiba/Jobin-Yvon HR800 Raman spectrometer with a 632.8 nm excitation laser wavelength. For collecting Raman spectra on solutions, the samples were kept in quartz cuvettes closed in a nitrogen atmosphere. PL spectra were corrected with transfer functions as described previously.[39]

X-ray fluorescence (XRF) was performed with a Fisher XAN 250 instrument that utilized a voltage of 50 kV, a silicon drift detector, a primary nickel filter, and helium as a flowing gas

purge. For XRF measurements, the complexes were sealed in mylar packets under a nitrogen atmosphere.

Proton Nuclear Magnetic Resonance (^{1}H-NMR) was performed with a Bruker AVIII-400-HD instrument using a relaxation time of 6 s and 16 scans. Deuterated dimethyl sulfoxide was used as the solvent. For quantitative measurements ethylene carbonate was added as an internal standard.

X-ray diffraction (XRD) was performed with a Rigaku SmartLab diffractometer using a Cu Kα (λ = 1.5406) source and operated at 40 kV and 44 mA in parallel beam mode.

Mass spectrometry analysis was performed with electrospray ionization high-resolution tandem mass spectrometry (ESI/HRMS/MS) experiments by using a Thermo Scientific LTQ Orbitrap XL hybrid mass spectrometer. The solutions were infused into the ESI source at a rate of 5-7 µL min^{-1} using a syringe pump. The ESI source conditions were set as follows: 3 kV spray voltage, 40 (arbitrary units) flow rate of sheath gas (N_2), 10 (arbitrary units) flow rate of auxiliary gas (N_2), and 275 °C capillary temperature. Voltages for the ion optics were optimized using the tuning features of the LTQ Tune Plus interface. Mass spectra were collected in both negative- and positive-ion modes. Elemental compositions were obtained via high-resolution mass analysis by using the orbitrap and were further confirmed based on isotopic distribution patterns and collision-activated dissociation (CAD) mass spectra. When isolated and subjected to CAD, both the indium polyselenide and copper polyselenide anions underwent losses of selenium atoms (representative examples shown in Figures S1 and S2). Samples were prepared under a nitrogen atmosphere to minimize potential exposure to oxygen and moisture.

Inductively coupled plasma optical emission spectroscopy (ICP-OES) was performed with an iCAP 7400 ICP-OES analyzer after digestion in trace-element nitric acid. Standards were made by dissolving the respective elements in nitric acid and diluting with ultrapure water.

Transmission electron microscopy (TEM) was performed using a Tecnai G2 20 TEM at an accelerating voltage of 200 kV.

X-ray absorption spectroscopy (XAS) measurements were conducted at the 10-BM-B beamline at the Advanced Photon Source (APS) of Argonne National Laboratory (ANL), at the In K (27940 eV), Se K (12658 eV), and Cu K (8979 eV) edge in transmission mode, with an energy resolution of 0.5 eV and edge energy precision greater than 0.1 eV. The samples were sealed in liquid cells designed for XAS analysis and were scanned at room temperature. Each measurement was accompanied by simultaneous acquisition of foil absorption spectra obtained through a third ion chamber for energy calibration. XAS data were fit using winXAS3.1. Least-squares regression fits of the k^2-weighted Fourier transform data from 2.5 to 11.5 Å^{-1} in k-space were used to obtain the extended x-ray absorption fine structure (EXAFS) coordination parameters. The first shell was used to fit all spectra. All samples were fit using theoretical scattering paths using FEFF. The S_o^2 values were 0.65 for the In edge, 0.95 for the Se edge, and 0.70 for the Cu edge as determined by fitting In foil, bulk Se, and Cu foil, respectively.

Current−voltage (JV) measurements were done at standard AM1.5 conditions with an Oriel Sol3A solar simulator at 25 °C.

Safety Consideration

Care should be taken when working with several chemicals used in this procedure. Amines are known to be corrosive and can cause skin and eye irritation. Ethanethiol is flammable and extremely malodorous. Care should also be taken with the n-alkylammonium polyselenides, we observe to be highly corrosive (expanded upon below for the use of reactive dissolution of metals). Further, the potential for toxic H_2Se formation from the polyselenides should be considered.

Results and discussion

n-Alkylammonium Polyselenide Synthesis and Isolation

Selenium has been shown to dissolve in various combinations of an amine and a thiol.[40–42] In previous research by our group, we investigated the different types of soluble selenium-containing compounds that form in these solutions.[43] Through various characterization techniques, it was confirmed that when selenium is dissolved in a monoamine-monothiol solution, it will produce an n-alkylammonium polyselenide ($(R_1NH_3)_2Se_x$ where x varies based on amine:thiol ratio) and a disulfide (R_2SSR_2).[43]

In the search for a selenium-based alkahest, n-alkylammonium polyselenides pose an interesting option. First, they possess a structural that is analogous to the n-alkylammonium dithiolates that have been identified as key intermediates in amine-thiol reactive dissolution chemistry.[23] Second, the presence of these n-alkylammonium polyselenides in monoamine-monothiol solutions allowed for the dissolution of tellurium, which is otherwise insoluble in monoamine-monothiol alone. Furthermore, Se-Te bonding was observed with no evidence of S-Te bonding, suggesting that the n-alkylammonium polyselenide species itself facilitated the dissolution of tellurium.[43] Together, these observations lead us to investigate if n-alkylammonium polyselenides may have broader applicability in reactive dissolutions, thereby providing a selenium-based alkahest that is analogous to the amine-thiol system.

To evaluate the potential of an n-alkylammonium polyselenide system independent of any sulfur-containing compounds, these n-alkylammonium polyselenides must first be separated from any thiols or disulfides. To achieve this, n-butylamine (BA) and ethanethiol (ET) were used to synthesize n-butylammonium polyselenide (BAPSe), which was subsequently separated through precipitation with toluene and cyclohexane. Through ^{1}H-NMR analysis (Figure 2a) no thiol or disulfide compounds were observed after the isolation and redissolution of the BAPSe. Elemental analysis of the dried BAPSe with XRF clearly showed the presence of selenium with no detectable sulfur (Figure 2b). These observations show that the precipitation and washing procedure is successful at separating the BAPSe from the thiols and disulfides in the initial synthesis solution. The BAPSe was then redissolved in n-

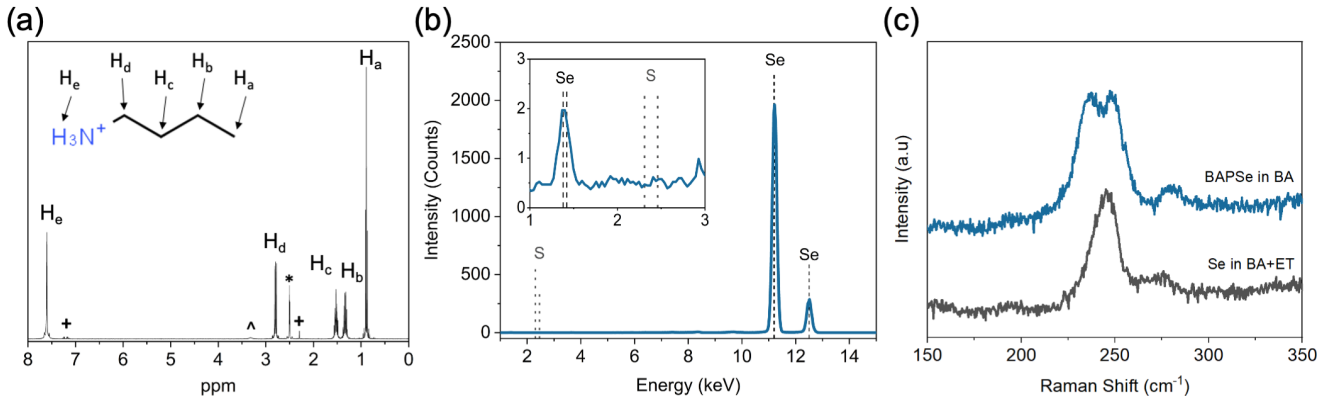

Figure 2. (a) ^{1}H-NMR of the isolated butylammonium polyselenide shows no evidence of thiols. Peaks marked with * are due to deuterated dimethyl sulfoxide, peaks marked with ^ are due to H_2O in the deuterated solvent, and peaks marked with + represent residual toluene from the isolation procedure. (b) XRF spectrum of dried butylammonium polyselenide. (c) Raman spectra of selenium dissolved in a n-butylamine-ethanethiol solution (gray) and a solution of the isolated n-butylammonium polyselenide redissolved in n-butylamine (blue).

butylamine or polar solvents, such as dimethylformamide. Note that to obtain sulfur-free solutions of n-alkylammonium polyselenides in this study, we used the combination of monoamines and thiols for the dissolution of selenium. In our previous study, we demonstrated that the use of diamine-thiol mixtures could result in polyselenides bound to the thiolates.[43]

A comparison between the Raman spectra of selenium dissolved in n-butylamine and ethanethiol and for BAPSe dissolved in n-butylamine provides interesting insights into changes in the structure of the polyselenide ions. In the n-butylamine-ethanethiol solution, a Se-Se band was detected at approximately 245 cm^{-1}. However, after precipitation, two Se-Se peaks were detected at 237 cm^{-1} and 249 cm^{-1} (Figure 2c). The position of the Se-Se peak has been reported to change both with the number of Se atoms (x) in a polyselenide compound and the structure of the polyselenide ions, be it linear or cyclic.[43] For linear polyselenide ions, a larger Raman shift would correspond to a shorter chain length, while for cyclic polyselenide ions the Raman shift does not vary linearly with size, but Se_6 and Se_8 rings are expected to cause peaks at 247 cm^{-1} and 249 cm^{-1}, respectively.[43] However, Kanatzidis et al. suggest that in solution, polyselenide ions tend to exist in a linear form.[16] This leads us to the conclusion that the observed peaks at 237 cm^{-1} and 249 cm^{-1} are attributed to two different lengths of polyselenide chains. Additionally the peak at 280 cm^{-1} has been previously observed in other polyselenide solutions and may be related to a different vibrational mode of the Se-Se bonds.[43] Further, no evidence of S-S, C-S, or S-Se bonding is observed at higher Raman shifts (Figure S3).

To better understand the size of the polyselenide ions in the BAPSe used in this work, measurements of the average polyselenide chain length was made indirectly by determining the ratio of butylammonium to selenium and assuming a composition of two butylammonium ions per polyselenide chain based on charge balance arguments. Quantitative ^{1}H-NMR measurements on a known mass of the isolated, solid BAPSe sample, dissolved in deuterated DMSO, allowed for the determination of the mass percent of any hydrogen containing components in the sample. This analysis revealed the presence of n-butylammonium and toluene. By comparing the peak integration to that of the ethylene carbonate internal standard, n-butylammonium was found to make up 23.8±0.2% by mass. Meanwhile, residual toluene from the isolation procedure was found to make up 16±1% by mass. Therefore, selenium corresponds to about 60% by mass if all remaining mass is attributed to selenium. To validate this analysis, ICP-OES was used to determine the mass percent of selenium in the sample. This came out to be 62%, in good agreement with the quantitative ^{1}H-NMR results. We also note that in the ICP-OES measurements, no sulfur was observed above the baseline, supporting the previous XRF measurements. All put together, this method estimates that the average value for x in the Se_x^{2-} compounds was just below 5. While information on the average size is a useful reference, it is unlikely that a solution of BAPSe in n-butylamine contains polyselenide ions of homogenous size. Not only do the Raman spectra signal the possibility of two distinct compounds, but in general, polyselenide solutions are at a dynamic equilibrium and will react with each other to exchange selenium atoms, producing some larger and smaller polyselenide ions.[17]

Reactive Dissolution of Metals with n-Alkylammonium Polyselenide Solutions

To determine the reactive dissolution capabilities of n-alkylammonium polyselenides, solutions of BAPSe in n-butylamine were used to dissolve a range of different metals. After allowing reactions to occur, insoluble compounds were separated via centrifugation and the remaining solution that contained the soluble compounds was then drop-cast and annealed. The compositions of the resulting films were qualitatively analyzed via XRF. Many of the targeted elements were detected including copper, indium, silver, zinc, cadmium, germanium, tin, and arsenic, indicating that each had some solubility in n-alkylammonium polyselenide solutions. Attempts to dissolve elemental lead, bismuth, and antimony were unsuccessful. The ratio of selenium to metal is an important factor in dictating the total amount of metal that can be

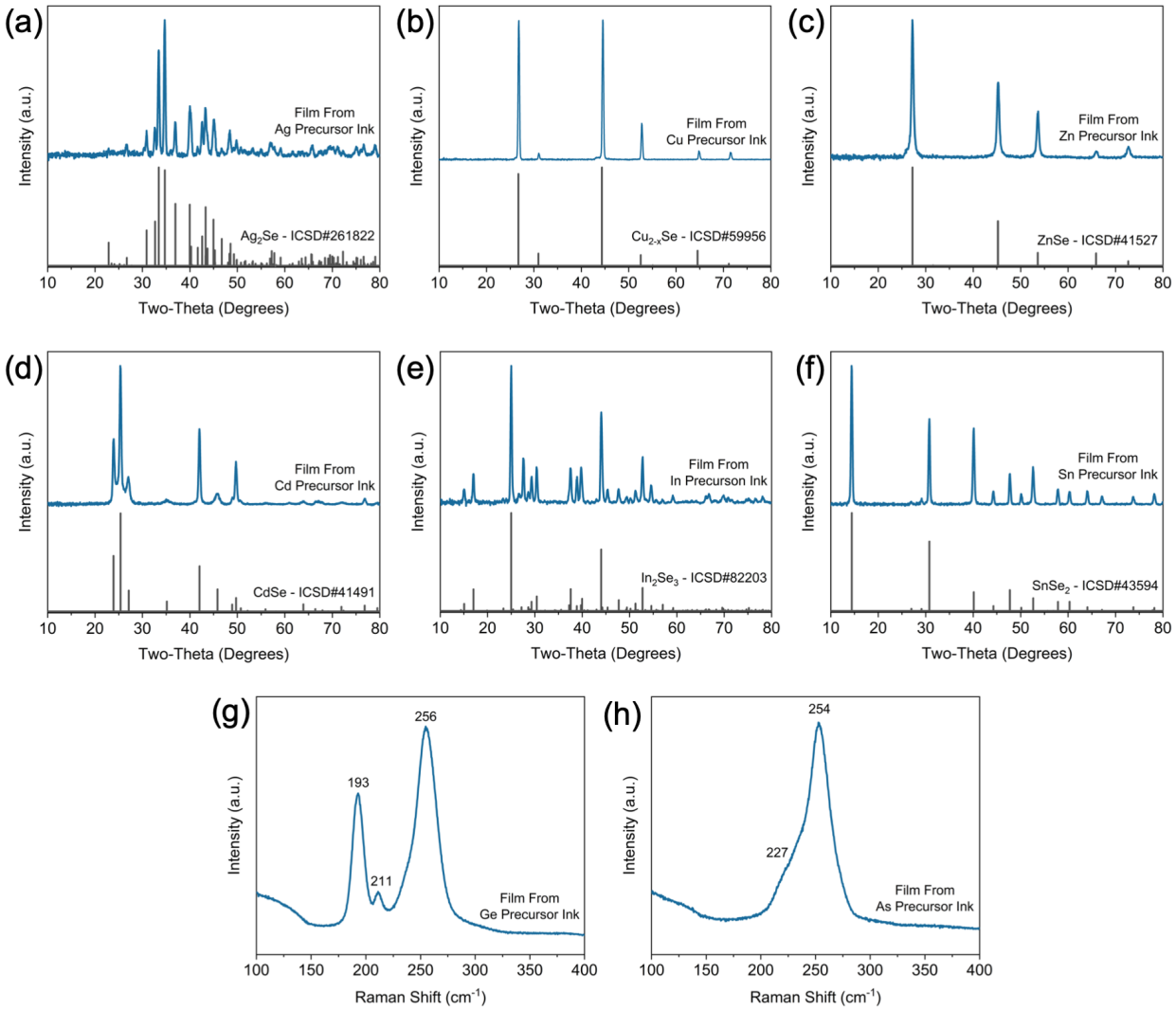

Figure 3. XRD patterns of the binary selenides made by heating films coated with inks made from a) Ag in BAPSe+BA, b) Cu in BAPSe+BA, c) Zn in BAPSe+BA, d) Cd in BAPSe+BA, e) In in BAPSe+BA, and f) Sn in BAPSe+BA. Raman spectra showing the metal chalcogenide glasses made by heating films coated with inks generated from g) Ge in BAPSe+BA and h) As in BAPSe+BA.

solubilized. It should be noted that when using a ratio of 10 selenium atoms for each metal atom, copper, indium, arsenic, and tin were fully dissolved. Silver was fully dissolved by using 20 selenium atoms per silver atom. It should be noted that the solutions were stored in an inert atmosphere to prevent potential reactions with H_2O or O_2. Under these conditions, the solutions appeared stable for months.

As a proof of concept, the inks containing dissolved metals were used to make solution-processed metal selenides by a drop-casting and annealing technique. The XRD patterns (Figure 3) for films obtained from inks containing silver, copper, zinc, cadmium, indium, and tin showed crystallinity as they had decomposed into silver(I) selenide, copper(I) selenide, zinc(II) selenide, cadmium(II) selenide, indium(III) selenide, and tin(IV) selenide, respectively. The films generated from germanium and arsenic inks were amorphous. Raman spectroscopy analysis (Figure 3) revealed the formation of selenium-rich metal chalcogenide glasses.[44,45]

The same procedure was also used to successfully dissolve copper metal in a hexylammonium polyselenide solution and a propylammonium polyselenide solution. Altering the alkylammonium chain length did not produce any apparent change in the dissolution time. Alternatively, BAPSe was synthesized and then redissolved in DMF as an alternative polar solvent. Again, no apparent change in ability to serve as a reactive solvent system was observed.

Reactive dissolutions with n-alkylammonium polyselenide solutions are not limited to metals. We also learned that BAPSe solutions can dissolve Cu_2O and Cu_2Se (Figure S4), which are generally insoluble in amines alone. BAPSe solutions can also be used to dissolve metal halides. However, because most metal halides are soluble in polar solvents, it was less obvious if the polyselenides had reacted with the metal halides. To study this, Raman spectra were collected for solutions of $InCl_3$ in DMF with and without BAPSe. When no BAPSe was used, a peak corresponding to In-Cl vibrations was seen at 294 cm^{-1}. When BAPSe was present, this In-Cl vibration was no longer observed. Instead, peaks corresponding to In-Se vibrations were noted at 173 cm^{-1} and 190 cm^{-1}, indicating that the BAPSe did react with the $InCl_3$ precursor to form a new compound (Figure S5).

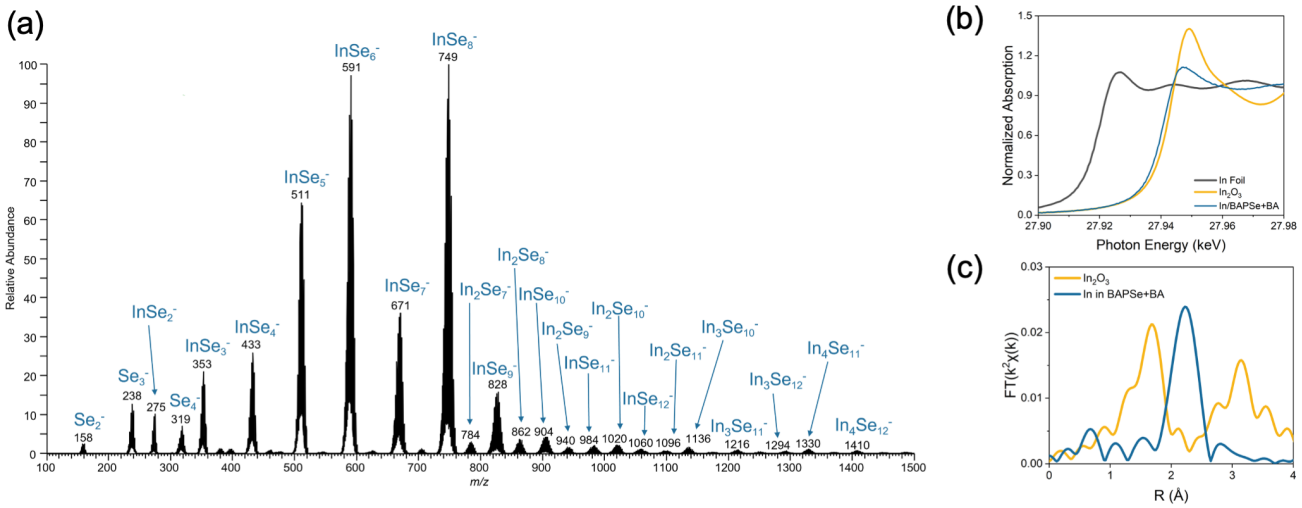

Figure 4. a) Negative-ion mode ESI/MS spectra, b) XANES spectra, and c) EXAFS spectra at indium edge for indium dissolved in BAPSe+BA.

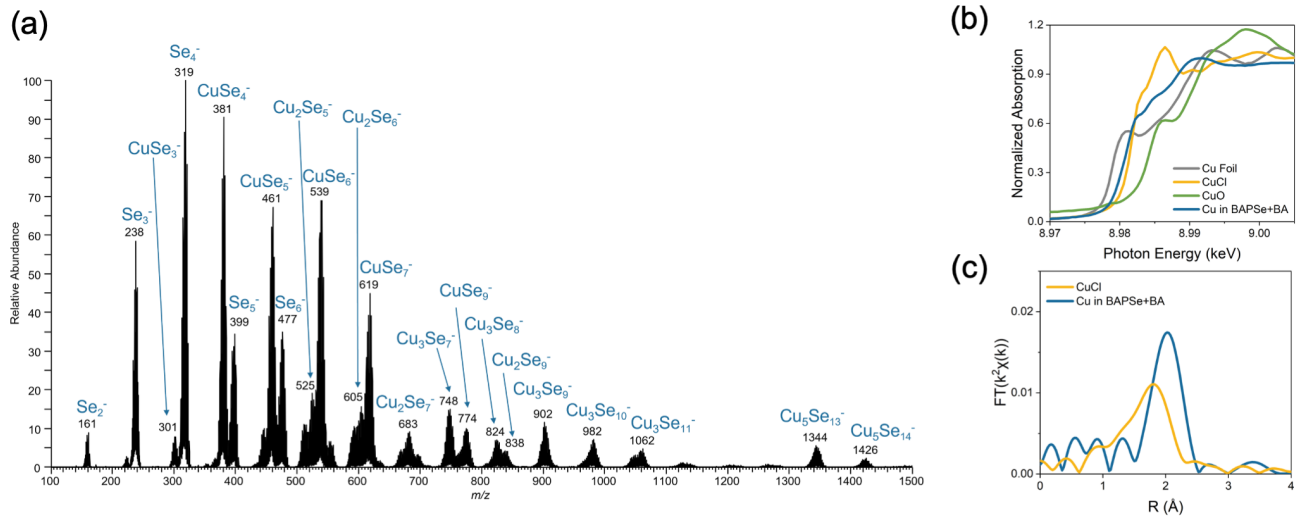

Figure 5. a) Negative-ion mode ESI/MS spectra, b) XANES spectra, and c) EXAFS spectra at copper edge for copper dissolved in BAPSe+BA.

We also found that cations other than n-alkylammoniums can be used. Hydrazine is known to dissolve selenium via a reaction that forms hydrazinium polyselenide.[24] While the hydrazine-chalcogen reactive solvent system has been studied extensively, it has been used to dissolve metal chalcogenides via dimensional reduction.[22] For example, for high efficiency $Cu(In,Ga)(S,Se)_2$ solar cells, In_2Se_3 is used as the indium source and dissolved with hydrazine and selenium.[46] In this work we found that hydrazinium polyselenide solutions in hydrazine can directly dissolved indium metal (Figure S6), distinct from what has been reported previously. This opens the door that other inorganic cations may also be possible, lending further ability to modify this polyselenide reactive dissolution chemistry.

Mechanism of Reactive Dissolution with Polyselenides

It is clear that n-alkylammonium polyselenide solutions are powerful reactive solvent systems capable of solubilizing a wide range of precursors. Ultimately, having a general theory to explain this reactive dissolution chemistry would provide predictive ability that could guide targeted synthesis. However, this level of understanding tends to be challenging in alkahest chemistry due to the complicated nature of the reactions. Successful solvation relies on both the ability of the solvent system to react with the target solute and on the solubility of the newly formed molecule in the general solution. To date, a general predictive theory has evaded researchers in the similar amine-thiol chemistry. However, understanding how metals are oxidized by this reactive solvent system and what chemical structures form upon reaction would be a first step in developing a deeper understanding of this chemistry.

ESI/MS was used to analyze solutions of indium metal dissolved with BAPSe in n-butylamine, where ions were identified by their mass/charge ratio and isotopic distribution patterns, and further supplemented by collision-activated dissociation mass spectra where needed. The negative-ion

mode ESI/MS analysis revealed the presence of ions containing indium and selenium, as well as a few ions that only contain selenium (Figure 4a). Positive-ion mode ESI/MS analysis revealed the typical ions expected for n-butylamine or n-butylammonium cations (Figures S7 and S8). These findings suggest that indium reacts with BAPSe to form n-butylammonium indium polyselenide compounds. Analysis of copper metal dissolved in BAPSe in n-butylamine (Figure 5a) likewise showed the presence of compounds containing only copper and selenium, suggesting the formation of n-butylammonium copper polyselenides.

X-ray absorption spectroscopy (XAS) was performed to gain further insight into the metal polyselenides. For this analysis, five key parameters were fit: amplitude reduction factor (S_0^2), coordination number (CN), bond distance (R), Debye-Waller factor (σ^2), and edge energy (E_0). Reference materials were measured to verify oxidation states. Through a combination of X-ray absorption near edge structure (XANES) and extended X-ray absorption fine structure (EXAFS), it was determined that after reactions with BAPSe, the indium was in the +3 oxidation state and bound to selenium with a coordination number of approximately 6 (Figures 4a & 4b). The same analysis indicated that copper was in the +1 oxidation state and bound to selenium with a coordination number of approximately 4 (Figures 5a & 5b). Further details of the XAS analysis can be found in the SI.

As mentioned above, a monoamine-dithiol solvent system is a similarly powerful reactive solvent system. For that system, the proposed reaction mechanism for the dissolution of metals begins with the amine deprotonating the thiol to form an n-alkylammonium dithiolate.[23] There is an interesting structural similarity between n-alkylammonium polyselenides and n-alkylammonium dithiolates as both involve an n-alkylammonium cation and a chalcogen-terminated anion. This suggests that a similar reaction mechanism may exist for both solvent systems. In the case of the monoamine-dithiol solvent system, the oxidation of the metals provides electrons that liberate hydrogen gas from the n-alkylammonium cation, converting it back into an n-alkylamine.[23] In monoamine-dithiol metal dissolutions, reactions are often fast enough that the bubbling of liberated hydrogen can be observed. Additionally, the formation of hydrogen can be observed through the use of thermal conductivity detection mass spectrometry (TCD/MS).[23] However, for the BAPSe dissolution of copper and indium, no visible bubbling was observed and TCD/MS measurements of the headspace gas from the dissolution vials revealed no release of hydrogen (Figure 6a). This suggests that alkylammonium polyselenide reactive dissolution is not undergoing an analogous mechanism compared to the amine-thiol reactive solvent system.

If the oxidation of the metals does not lead to the release of hydrogen via reduction of protons, the next logical option would be reduction of the polyselenide ions. This could occur by splitting one larger polyselenide chain into two smaller polyselenide chains. These smaller polyselenide chains could then bind to the oxidized metals to form the metal polyselenide ions. Evidence for this reaction occurring can be obtained through Raman analysis (Figure 6b). As discussed above, the

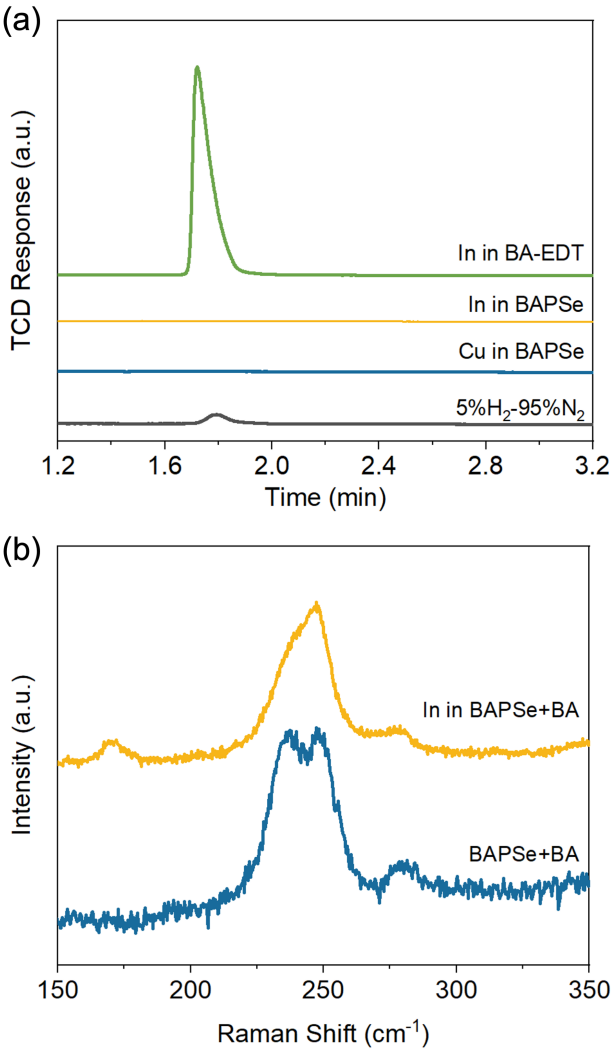

Figure 6. a) TCD response of the headspace gas in amine-thiol and butylammonium polyselenide metal dissolutions compared to a $5\%H_2$-$95\%N_2$ mixture and b) Raman spectrum of Indium dissolution in BAPSe+BA (yellow) compared to the BAPSe+BA spectra previously shown in Figure 2c (blue).

isolated BAPSe showed two Raman peaks related to Se-Se bonding, with the peak at lower Raman shift corresponding to longer polyselenide chains. Analysis after the dissolution of indium showed the emergence of a new peak at around 173 cm^{-1} that can be attributed to In-Se bonding.[24,47] Interestingly, a notable difference was also detected in the relative intensities of the Se-Se peaks. Following the reaction, the peak corresponding to longer Se chain lengths had decreased in magnitude relative to the peak corresponding to shorter Se chain lengths. A similar trend is also observed for the dissolution of Cu metal, and to a lesser extent the dissolution of Ag metal (Figure S9). This finding may indicate the breakdown of longer chains into shorter chains, supporting the proposed oxidation of metals via reduction of polyselenide chains into smaller chains. Additionally, the BAPSe can also dissolve more elemental selenium. In this case, the opposite trend is observed where the peak that corresponds to longer Se chain lengths

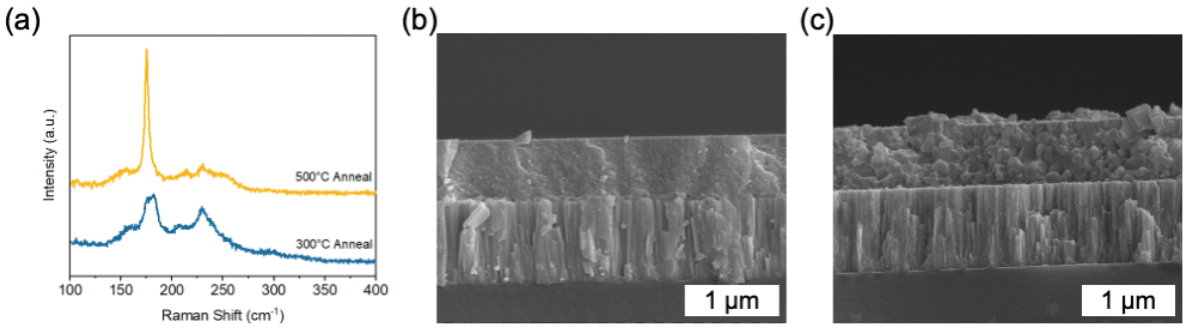

Figure 7. a) Raman spectra of solution-processed $CuInSe_2$ films made using inks containing copper and indium metal dissolved in BAPSe+BA and annealed at 300 °C (blue) and 500 °C (yellow), b) SEM image of film annealed at 300 °C for 2 min following each coating, c) SEM image of film annealed at 500 °C for 20 minutes.

increases relatively (Figure S10). This could indicate that the ability of BAPSe to dissolve additional selenium does so by increasing the length of the polyselenide chains.

This hypothesis is further supported by XAS analysis at the Se K edge for In dissolutions in BAPSe (Figure S11). With an increasing amount of indium dissolved, the coordination number for Se-Se bonds decreases. This reduced Se-Se CN is consistent with the breaking of Se-Se bond via reduction of the polyselenide chains. For example, in a Se_2^{2-} chain, the average Se-Se CN would be 1. On the other hand, in a linear Se_8^{2-} chain, the average Se-Se CN would be 1.75. While this technique is not precise enough to confidently back-calculate the actual polyselenide chain length, the general trend is indicative that oxidation of metals occurs due to the reduction of larger polyselenide chains into smaller polyselenide chains.

Further work is needed to determine how this reaction mechanism might change when starting with an already oxidized metal source but is discussed in the SI for reactions of $InCl_3$ with BAPSe.

Application to Solution-Processed Multinary Selenides

While we have already shown that the n-alkylammonium polyselenide reactive solvent system can be used to generate inks for solution-processed binary metal selenides, this method also holds promise for multinary metal selenides. $CuInSe_2$ (CISe) is an important material for photovoltaic applications as it has a bandgap of approximately 1 eV and is a promising option as the bottom absorber in tandem photovoltaics.[48] With the ability to dissolve copper and indium with BAPSe in n-butylamine, the n-alkylammonium polyselenide system offers a direct molecular precursor route to CISe. Inks containing the respective metals were combined and used to coat films that were annealed at 300 °C for 5 minutes following each coating. Raman analysis (Figure 7a) showed the presence of CISe with the broad peak around 180 cm^{-1} which can be attributed to the A_1 vibrational mode, with potential shift from the expected location of 175 cm^{-1} due to the presence of defects.[49] Additionally, the ordered vacancy compound, $CuIn_3Se_5$, commonly observed on the surface of CISe materials is evidenced by the peak at about 158 cm^{-1}. Additional free selenium may be present in the films as evidenced by the magnitude of the peak at 230 cm^{-1}, though this peak overlaps with the E/B_2 modes of CISe with peaks occurring at 210 cm^{-1} and 230 cm^{-1}.[50] The broad nature of the Raman bands indicates a nanocrystalline nature of the material, which

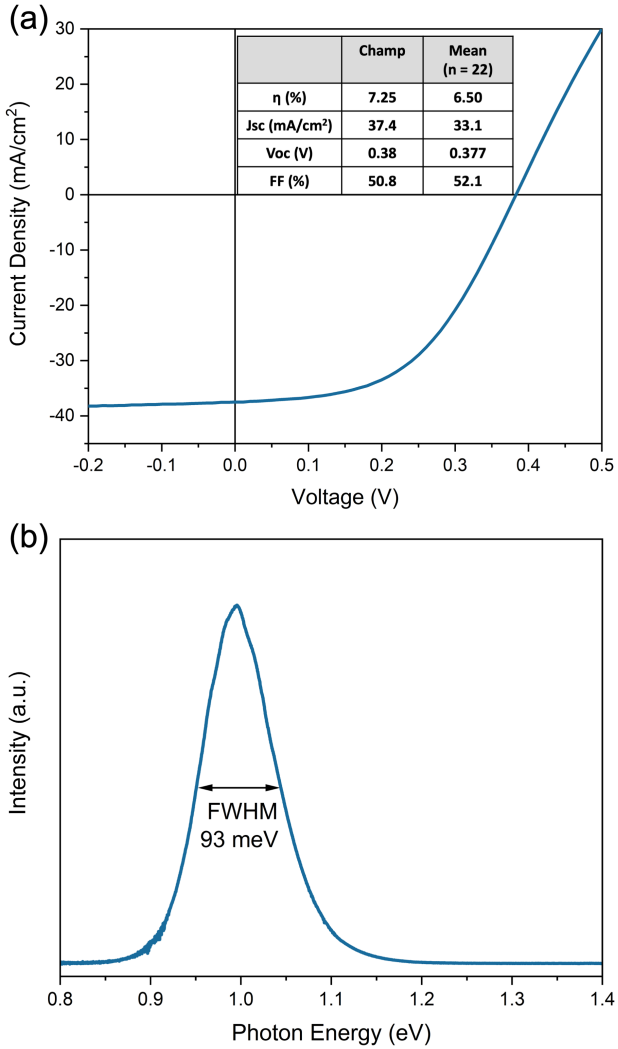

Figure 8. a) JV curve for the champion $CuInSe_2$ solar cell made from polyselenide ink with inset table comparing to average cell performance and b) PL spectrum from champion $CuInSe_2$ solar cell.

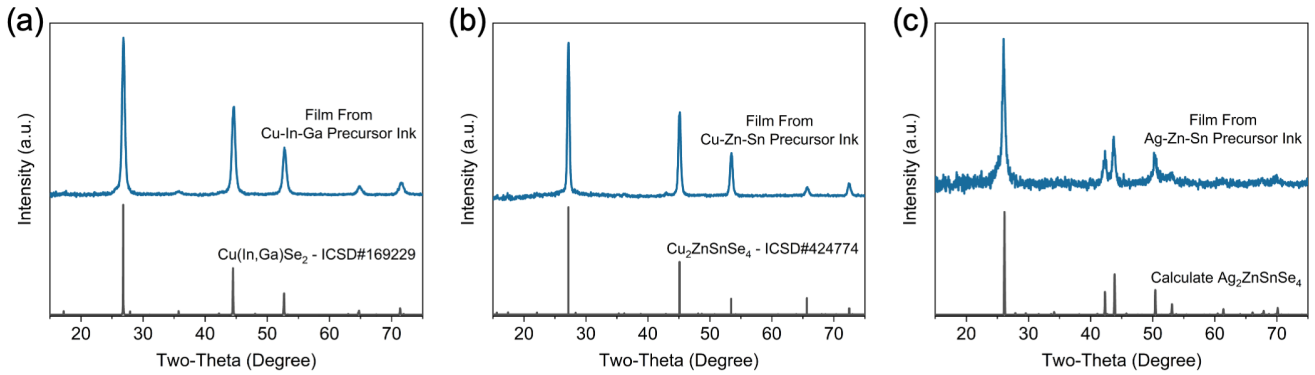

Figure 9. a) XRD pattern of $Cu(In,Ga)Se_2$ film made using ink containing copper, indium, and gallium metals dissolved in BAPSe+BA, b) XRD pattern of $Cu_2ZnSnSe_4$ film made using ink containing copper, zinc, and tin metals dissolved in BAPSe+BA, and c) XRD pattern of $Ag_2ZnSnSe_4$ film made using ink containing silver, zinc, and tin metals dissolved in BAPSe+BA.

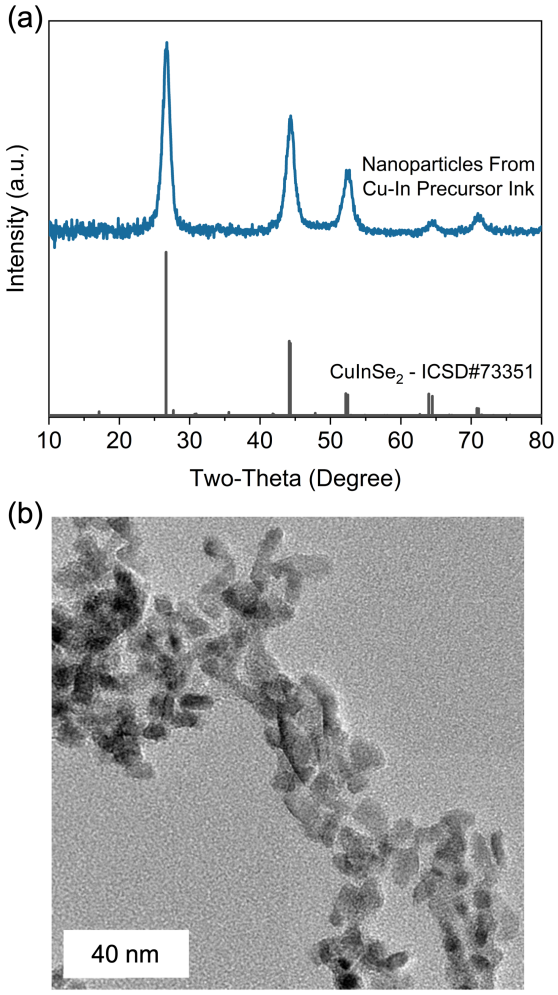

Figure 10. a) XRD pattern and b) TEM image of nanoparticles made using ink containing copper and indium metals dissolved in BAPSe+BA.

was confirmed via SEM (Figure 7b). The films were subsequently annealed at 500 °C for 20 minutes to induce further grain growth. This resulted in a sharpening of the main CISe A_1 Raman peak and a shift to 175 cm^{-1}, which suggests that the grain size increased and the amount of defects decreased during annealing (Figure 7a). A relative reduction in intensity of the peak at 230cm^{-1} indicates the removal of free selenium, though the overlap with the E/B_2 modes of CISe make it difficult to determine whether free selenium had been fully removed. SEM confirmed the increase in apparent grain size (Figure 7c).

Further, we utilized Cu_2Se- and In-containing polyselenide inks to fabricate films for complete solar cells. Following blade coating, a heat treatment in a Se-containing atmosphere was used to coarsen the grains. Solar cells with an average of 6.5% (active area) efficiency were obtained, with the champion device at 7.25% (Figure 8a). Data on individual cell parameters can be found in the SI (Table S2 and Figure S12). Furthermore, photoluminescence measurements on the champion cell confirmed the optoelectronic quality of the CISe absorber layer showing strong emission centered just below 1 eV with a full width at half max of around 93 meV (Figure 8b). Similar PL spectra were obtained for other cells processed in the same way (Figure S13). This shows that inks based on alkylammonium polyselenide chemistry are able to obtain the material and optoelectronic properties needed to produce functioning solar cells. Further improvement in the device efficiency is likely to be obtained with more optimization of the heat treatment steps as this can play a major role in defect formation.

While CISe is useful in tandem applications, alloying with gallium allows for the bandgap to be tuned, thus making it a highly efficient absorber in single junction photovoltaics.[51] However, gallium on its own was not observed to have any solubility in n-alkylammonium polyselenide solutions. A similar challenge exists for the amine-thiol solvent system, but has been bypassed through the observation that gallium metal can dissolve in monoamine-dithiol solutions if indium is also present.[52,53] The same strategy was found to facilitate the dissolution of gallium with n-alkylammonium polyselenides. This allows for the creation of an n-alkylammonium polyselenide ink containing copper, indium, and gallium. A film was cast from this ink and subsequently annealed at 400 °C for 5 minutes. XRD of the resulting film (Figure 9a) shows the presence of chalcopyrite $Cu(In,Ga)Se_2$ (CIGSe) with no secondary phases. The presence of gallium in the crystal structure causes the obtained XRD spectrum to be slightly shifted relative to $CuInSe_2$. To the best of our knowledge, this is

the first solution-processed, sulfur-free CIGSe film made directly by a molecular precursor approach.

Additionally, such a wide range of soluble metal-selenium complexes allows for solution deposition of other various ternary and quaternary metal selenides. The $Cu_2ZnSn(S,Se)_4$ materials system has been considered a promising earth-abundant alternative to CIGSe.[54] However, defects in $Cu_2ZnSnSe_4$ have led researchers to investigate substituted alternatives such as $Ag_2ZnSnSe_4$.[55] While efficiencies of $Cu_2ZnSn(S,Se)_4$ solar cells were stagnant below 13% for many years, recent breakthroughs have allowed for $(Ag,Cu)_2ZnSn(S,Se)_4$ device efficiencies above 14% and may usher in a renewed interest in these materials.[28,56] By combining copper or silver with zinc and tin in polyselenide inks at an appropriate stoichiometry, pure selenide $Cu_2ZnSnSe_4$ and $Ag_2ZnSnSe_4$ were produced through drop-cast methods. XRD (Figure 9) was used to identify the materials and confirm the absence of secondary phases.

Beyond directly coating thin films from molecular precursors, metal selenide nanoparticles are also of interest. The same precursor inks that were used to coat thin films can similarly be utilized as the metal and selenium source in nanoparticle reactions. Not only can binary copper selenide and green-fluorescent nanorods of indium selenide be made (Figure S14), but copper and indium dissolved with BAPSe can be used to synthesize ternary $CuInSe_2$ nanoparticles. The copper and indium polyselenides were isolated from excess n-butylamine through precipitation with toluene and redissolved in oleylamine. The solution was then allowed to react at 225°C for 30 minutes in a sealed vessel in a microwave reactor. The resulting nanoparticles were identified as chalcopyrite $CuInSe_2$ through XRD (Figure 10a) with TEM showing a size of around 10 nm (Figure 10b).

Conclusions

This work introduces a selenium-based “alkahest” in the form of n-alkylammonium polyselenide solutions. These solutions are shown to be capable of dissolving a wide range of metals, including Cu, Ag, Zn, Cd, In, Ga, Sn, Ge, and As, and metal oxides, metal chalcogenides, and metal halides. This reactive dissolution of metals produces soluble n-alkylammonium metal polyselenides, hypothesized to occur by oxidizing the metals through the reduction of polyselenide ions. This route provides a convenient method for synthesizing soluble metal-selenium bonded complexes that can subsequently be used to produce solution-processed metal selenides. Not only can pure binary metal selenides be produced, but we have also shown that by combining inks, pure multinary metal selenides like $Cu(In,Ga)Se_2$, $Cu_2ZnSnSe_4$, and $Ag_2ZnSnSe_4$ can be synthesized.

Conflicts of interest

There are no conflicts to declare.

Acknowledgements

The authors are appreciative of financial support from the National Science Foundation with Grants 1735282-NRT (SFEWS) and 10001536 (INFEWS). Use of the Advanced Photon Source was supported by the U.S. Department of Energy Office of Basic Energy Sciences under contract no. DE-AC02-06CH11357. MRCAT operations, beamlines 10-BM, is supported by the Department of Energy and the MRCAT member institutions.

Notes and references

1 S. M. McLeod, C. J. Hages, N. J. Carter and R. Agrawal, Synthesis and characterization of 15% efficient CIGSSe solar cells from nanoparticle inks, *Prog. Photovoltaics Res. Appl.*, 2015, **23**, 1550–1556.

2 C. K. Miskin, S. D. Deshmukh, V. Vasiraju, K. Bock, G. Mittal, A. Dubois-Camacho, S. Vaddiraju and R. Agrawal, Lead Chalcogenide Nanoparticles and Their Size-Controlled Self-Assemblies for Thermoelectric and Photovoltaic Applications, *Appl. Nano Mater.*, 2019, **2**, 1242–1252.

3 D. V. Talapin and C. B. Murray, PbSe nanocrystal solids for n- and p-channel thin film field-effect transistors, *Science*, 2005, **310**, 86–89.

4 J. M. Caruge, J. E. Halpert, V. Wood, V. Bulovic and M. G. Bawendi, Colloidal quantum-dot light-emitting diodes with metal-oxide charge transport layers, *Nat. Photonics*, 2008, **2**, 247–250.

5 D. B. Mitzi, Solution-processed inorganic semiconductors, *J. Mater. Chem.*, 2004, **14**, 2355–2365.

6 S. Suresh and A. R. Uhl, Present Status of Solution-Processing Routes for $Cu(In,Ga)(S,Se)_2$ Solar Cell Absorbers, *Adv. Energy Mater.*, 2021, **11**, 2003743.

7 C. Coughlan, M. Ibáñez, O. Dobrozhan, A. Singh, A. Cabot and K. M. Ryan, Compound Copper Chalcogenide Nanocrystals, *Chem. Rev.*, 2017, **117**, 5865–6109.

8 Y. Min, G. Dae Moon, B. S. Kim, B. Lim, J.-S. Kim, Y. K. Chong and U. Jeong, Quick, Controlled Synthesis of Ultrathin Bi_2Se_3 Nanodiscs and Nanosheets, *J. Am. Chem. Soc*, 2012, **134**, 2872–2875.

9 B. Koo, R. N. Patel and B. A. Korgel, Synthesis of $CuInSe_2$ Nanocrystals with Trigonal Pyramidal Shape, *J. Am. Chem. Soc.*, 2009, **131**, 3134–3135.

10 K.-S. Cho, D. V Talapin, W. Gaschler and C. B. Murray, Designing PbSe Nanowires and Nanorings through Oriented Attachment of Nanoparticles, *J. Am. Chem. Soc.*, 2005, **127**, 7140–7147.

11 J. A. Clark, A. Murray, J.-M. Lee, T. S. Autrey, A. D. Collord and H. W. Hillhouse, Complexation Chemistry in N,N-Dimethylformamide-Based Molecular Inks for Chalcogenide Semiconductors and Photovoltaic Devices, *J. Am. Chem. Soc.*, 2018, **141**, 298–308.

12 S. W. Winslow, Y. Liu, J. W. Swan and W. A. Tisdale, Quantification of a PbClx Shell on the Surface of PbS Nanocrystals, *ACS Mater. Lett.*, 2019, **1**, 209–216.

13 B. Teymur, Y. Zhou, E. Ngaboyamahina, J. T. Glass and D. B.

Mitzi, Solution-Processed Earth-Abundant $Cu_2BaSn(S,Se)_4$ Solar Absorber Using a Low-Toxicity Solvent, *Chem. Mater.*, 2018, **30**, 6123.

14 R. Marin, A. Skripka, Y.-C. Huang, T. A. J. Loh, V. Mazeika, V. Karabanovas, D. H. C. Chua, C.-L. Dong, P. Canton and F. Vetrone, Influence of halide ions on the structure and properties of copper indium sulphide quantum dots, *Chem. Commun.*, 2020, **56**, 3341–3344.

15 M. D. Khan, M. A. Malik and N. Revaprasadu, Progress in selenium based metal-organic precursors for main group and transition metal selenide thin films and nanomaterials, *Coord. Chem. Rev.*, 2019, **388**, 24–47.

16 M. G. Kanatzidis and S. P. Huang, Coordination chemistry of heavy polychalcogenide ligands, *Coord. Chem. Rev.*, 1994, **130**, 509–621.

17 M. G. Kanatzidis, Soluble Polychalcogenides of the Late Transition and Main Group Elements, *Comments Inorg. Chem.*, 1990, **10**, 161–195.

18 S. Dhingra and M. G. Kanatzidis, The Use of Soluble Metal-Polyselenide Complexes As Precursors to Binary and Ternary Solid Metal Selenides, *Mater. Res. Soc. Symp. Proc.*, 1990, **180**, 825–830.

19 S. S. Dhingra and M. G. Kanatzidis, Polyselenide Chemistry of Indium and Thallium in Dimethylformamide, Acetonitrile, and Water. Syntheses, Structures, and Properties of the New Complexes $[In_2(Se_4)_4(Se_5)]^{4-}$, $[In_2Se_2(Se_4)_2]^{2-}$, $[In_3Se_3(Se_4)_3]^{3-}$, and $[Tl_3Se_3(Se_4)_3]^{3-}$, *Inorg. Chem.*, 1993, **32**, 1350–1362.

20 K. M. Koskela, M. J. Strumolo and R. L. Brutchey, Progress of thiol-amine 'alkahest' solutions for thin film deposition, *Trends Chem.*, 2021, **3**, 1061–1073.

21 J. Tan, X. Zhang, J. Suh, N. Ha, J. Lee, S. D. Tilley and W. Yang, Molecular ink-derived chalcogenide thin films: Solution-phase mechanisms and solar energy conversion applications, *Mater. Today Energy*, 2023, **34**, 101288.

22 D. B. Mitzi, Solution Processing of Chalcogenide Semiconductors via Dimensional Reduction, *Adv. Mater.*, 2009, **21**, 3141–3158.

23 X. Zhao, S. D. Deshmukh, D. J. Rokke, G. Zhang, Z. Wu, J. T. Miller and R. Agrawal, Investigating Chemistry of Metal Dissolution in Amine-Thiol Mixtures & Exploiting it towards Benign Ink formulation for Metal Chalcogenide Thin Films, *Chem. Mater.*, 2019, **31**, 5674–5682.

24 C.-H. Chung, S.-H. Li, B. Lei, W. Yang, W. W. Hou, B. Bob and Y. Yang, Identification of the Molecular Precursors for Hydrazine Solution Processed $CuIn(Se,S)_2$ Films and Their Interactions, *Chem. Mater*, 2011, **23**, 964–969.

25 W. Liu, D. B. Mitzi, M. Yuan, A. J. Kellock, S. J. Chey and O. Gunawan, 12% Efficiency $CuIn(Se,S)_2$ Photovoltaic Device Prepared Using a Hydrazine Solution Process, *Chem. Mater*, 2010, **22**, 1010–1014.

26 T. Zhang, Y. Yang, D. Liu, S. C. Tse, W. Cao, Z. Feng, S. Chen and L. Qian, High efficiency solution-processed thin-film $Cu(In,Ga)(Se,S)_2$ solar cells, *Energy Environ. Sci*, 2016, **9**, 3674.

27 D. B. Mitzi, L. L. Kosbar, C. E. Murray, M. Copel and A. Afzali, High-mobility ultrathin semiconducting films prepared by spin coating, *Nature*, 2004, **428**, 299–303.

28 W. Wang, M. T. Winkler, O. Gunawan, T. Gokmen, T. K. Todorov, Y. Zhu and D. B. Mitzi, Device Characteristics of CZTSSe Thin-Film Solar Cells with 12.6% Efficiency, *Adv. Energy Mater.*, 2014, **4**, 1301465.

29 D. H. Webber and R. L. Brutchey, Alkahest for V_2VI_3 Chalcogenides: Dissolution of Nine Bulk Semiconductors in a Diamine-Dithiol Solvent Mixture, *J. Am. Chem. Soc.*, 2013, **135**, 15722–15725.

30 R. Zhang, S. Cho, D. G. Lim, X. Hu, E. A. Stach, C. A. Handwerker and R. Agrawal, Metal–metal chalcogenide molecular precursors to binary, ternary, and quaternary metal chalcogenide thin films for electronic devices, *Chem. Commun.*, 2016, **52**, 5007–5010.

31 C. L. McCarthy and R. L. Brutchey, Solution processing of chalcogenide materials using thiol-amine '"alkahest"' solvent systems, *Chem. Commun.*, 2017, **53**, 4888.

32 J. Park, W. Yang, Y. Oh, J. Tan, H. Lee, R. Boppella and J. Moon, Efficient Solar-to-Hydrogen Conversion from Neutral Electrolytes using Morphology-Controlled Sb_2Se_3 Light Absorbers, *ACS Energy Lett.*, 2019, **4**, 517–526.

33 J. Park, W. Yang, J. Tan, H. Lee, J. W. Yun, S. G. Shim, Y. S. Park and J. Moon, Hierarchal Nanorod-Derived Bilayer Strategy to Enhance the Photocurrent Density of Sb_2Se_3 Photocathodes for Photoelectrochemical Water Splitting, *ACS Energy Lett.*, 2020, **5**, 136–145.

34 X. Zhang, W. Yang, W. Niu, P. Adams, S. Siol, Z. Wang and S. D. Tilley, Thiol-Amine-Based Solution Processing of Cu_2S Thin Films for Photoelectrochemical Water Splitting, *ChemSusChem*, 2021, **14**, 3967–3974.

35 S. D. Deshmukh, R. G. Ellis, D. S. Sutandar, D. J. Rokke and R. Agrawal, Versatile Colloidal Syntheses of Metal Chalcogenide Nanoparticles from Elemental Precursors using Amine-Thiol Chemistry, *Chem. Mater.*, 2019, **31**, 9087–9097.

36 S. D. Deshmukh, K. G. Weideman, R. G. Ellis, K. Kisslinger and R. Agrawal, Enabling fine-grain free 2-micron thick CISe/CIGSe film fabrication via a non-hydrazine based solution processing route, *Mater. Adv.*, 2022, **3**, 3293–3302.

37 S. Yuan, X. Wang, Y. Zhao, Q. Chang, Z. Xu, J. Kong and S. Wu, Solution Processed $Cu(In,Ga)(S,Se)_2$ Solar Cells with 15.25% Efficiency by Surface Sulfurization, *Appl. Energy Mater.*, 2020, **3**, 6785–6792.

38 P. B. Vartak and R. Y. Wang, Tin(IV) Methylselenolate as a Low Temperature SnSe Precursor and Conductive 'Glue' Between Colloidal Nanocrystals, *ChemNanoMat*, 2020, **6**, 442–450.

39 A. A. Pradhan, M. C. Uible, S. Agarwal, J. W. Turnley, S. Khandelwal, J. M. Peterson, D. D. Blach, R. N. Swope, L. Huang, S. C. Bart and R. Agrawal, Synthesis of $BaZrS_3$ and $BaHfS_3$ Chalcogenide Perovskite Films Using Single-Phase Molecular Precursors at Moderate Temperatures, *Angew. Chemie - Int. Ed.*, 2023, **62**, e202301049.

40 B. C. Walker and R. Agrawal, Contamination-Free Solutions of Selenium in Amines for Nanoparticle Synthesis, *Chem. Commun.*, 2014, **50**, 8331–8334.

41 D. H. Webber, J. J. Buckley, P. D. Antunez and R. L. Brutchey, Facile dissolution of selenium and tellurium in a thiol-amine solvent mixture under ambient conditions, *Chem. Sci.*, 2014, **5**, 2498.
42 US 9,630,845 B2, 2017.
43 S. D. Deshmukh, L. F. Easterling, J. M. Manheim, N. J. Libretto, K. G. Weideman, J. T. Miller, H. I. Kenttämaa and R. Agrawal, Analyzing and Tuning the Chalcogen−Amine−Thiol Complexes for Tailoring of Chalcogenide Syntheses, *Inorg. Chem.*, 2020, **59**, 8240–8250.
44 L. Mochalov, A. Logunov, A. Kitnis and V. Vorotyntsev, Plasma-Chemistry of Arsenic Selenide Films: Relationship Between Film Properties and Plasma Power, *Plasma Chem. Plasma Process.*, 2020, **40**, 407–421.
45 T. G. Edwards and S. Sen, Structure and Relaxation in Germanium Selenide Glasses and Supercooled Liquids: A Raman Spectroscopic Study, *J. Phys. Chem. B*, 2011, **115**, 4307–4314.
46 T. K. Todorov, O. Gunawan, T. Gokmen and D. B. Mitzi, Solution-processed Cu(In,Ga)(S,Se)$_2$ absorber yielding a 15.2% efficient solar cell, *Prog. Photovoltaics Res. Appl.*, 2013, **21**, 82–87.
47 H. Zhou, C.-J. Hsu, W.-C. Hsu, H.-S. Duan, C.-H. Chung, W. Yang, Y. Yang, H. P. Zhou, C. Hsu, W. Hsu, H. Duan, C. Chung, W. B. Yang and Y. Yang, Non-Hydrazine Solutions in Processing CuIn(S,Se)$_2$ Photovoltaic Devices from Hydrazinium Precursors, *Adv. Energy Mater.*, 2013, **3**, 328–336.
48 A. R. Uhl, J. K. Katahara and H. W. Hillhouse, Molecular-Ink Route to 13.0% Efficient Low-Bandgap CuIn(S,Se)$_2$ and 14.7% Efficient Cu(In,Ga)(S,Se)$_2$ Solar Cells, *Energy Environ. Sci.*, 2016, **9**, 130.
49 D. W. Houck, E. I. Assaf, H. Shin, R. M. Greene, D. R. Pernik and B. A. Korgel, Pervasive Cation Vacancies and Antisite Defects in Copper Indium Diselenide (CuInSe$_2$) Nanocrystals, *J. Phys. Chem. C*, 2019, **123**, 9544–9551.
50 S. Levcenko, H. Stange, L. Choubrac, D. Greiner, M. D. Heinemann, R. Mainz and T. Unold, Radiative recombination properties of near-stoichiometric CuInSe$_2$ thin films, *Phys. Rev. Mater.*, 2020, **4**, 064605.
51 G. M. Wilson, M. Al-Jassim, W. K. Metzger, S. W. Glunz, P. Verlinden, G. Xiong, L. M. Mansfield, B. J. Stanbery, K. Zhu, Y. Yan, J. J. Berry, A. J. Ptak, F. Dimroth, B. M. Kayes, A. C. Tamboli, R. Peibst, K. Catchpole, M. O. Reese, C. S. Klinga, P. Denholm, M. Morjaria, M. G. Deceglie, J. M. Freeman, M. A. Mikofski, D. C. Jordan, G. TamizhMani and D. B. Sulas-Kern, The 2020 photovoltaic technologies roadmap, *J. Phys. D. Appl. Phys.*, 2020, **53**, 493001.
52 D. Rokke, S. D. Deshmukh and R. Agrawal, A Novel Approach to Amine-Thiol Molecular Precursors for Fabrication of High Efficiency Thin Film CISSe/CIGSSe Devices, *Conf. Rec. IEEE Photovolt. Spec. Conf.*, 2019, 1813–1815.
53 R. G. Ellis, J. W. Turnley, D. J. Rokke, J. P. Fields, E. H. Alruqobah, S. D. Deshmukh, K. Kisslinger and R. Agrawal, Hybrid Ligand Exchange of Cu(In,Ga)S$_2$ Nanoparticles for Carbon Impurity Removal in Solution-Processed Photovoltaics, *Chem. Mater.*, 2020, **32**, 5091–5103.
54 X. Liu, Y. Feng, H. Cui, F. Liu, X. Hao, G. Conibeer, D. B. Mitzi and M. Green, The current status and future prospects of kesterite solar cells: a brief review, *Prog. Photovoltaics Res. Appl.*, 2016, **24**, 879–898.
55 T. Gershon, K. Sardashti, O. Gunawan, R. Mankad, S. Singh, Y. S. Lee, J. A. Ott, A. Kummel and R. Haight, Photovoltaic Device with over 5% Efficiency Based on an n-Type $Ag_2ZnSnSe_4$ Absorber, *Adv. Energy Mater.*, 2016, **6**, 1601182.
56 J. Zhou, X. Xu, H. Wu, J. Wang, L. Lou, K. Yin, Y. Gong, J. Shi, Y. Luo, D. Li, H. Xin and Q. Meng, Control of the phase evolution of kesterite by tuning of the selenium partial pressure for solar cells with 13.8% certified efficiency, *Nat. Energy*, 2023, **8**, 526–535.